

REPORTS

# Continental Physiography, Climate, and the Global Distribution of Human Population<sup>1</sup>

Christopher Small and Joel E. Cohen

*Lamont-Doherty Earth Observatory of Columbia University, Palisades, NY 10964, U.S.A. (small@LDEO.columbia.edu)/Laboratory of Populations, Rockefeller University, and Columbia Earth Institute and School of International and Public Affairs, 1230 York Ave., Box 20, New York, NY 10021-6399, U.S.A. (cohen@rockefeller.edu). 15 IX 03*

<sup>1</sup> This research was supported by the University Consortium for Atmospheric Research (UCAR) Visiting Scientist Program (to C. S.) and by the Columbia Earth Institute in connection with the NASA Socio Economic Data and Applications Center (SEDAC). C. S. gratefully acknowledges the support of the Palisades Geophysical Institute and the Doherty Foundation. J. E. C. acknowledges with thanks the support of U.S. National Science Foundation grant DEB9981552 and the hospitality of Mr. and Mrs. William T. Golden during this work.

---

The spatial distribution of the global human population shows large variations over a wide range of spatial scales and population densities. Understanding what determines this distribution is fundamental to understanding the relationships between humans and the environment. These relationships have long been considered from the standpoint of both the physical system's influence on humans (e.g., Semple 1911; Huntington 1915, 1921, 1924, 1927, 1951, 1963; King, Bailey, and Sturdy 1994) and human influence on the rest of the system (see Vernadsky 1929, Vitousek et al. 1997, Kates, Turner, and Clark 1990 for an overview of perspectives on human-Earth relations). A necessary first step to understanding the spatial distribution of the population is to quantify its relationship to other factors that may influence it. While some qualitative observations of these relationships are well known, it has only recently become feasible to conduct quantitative analyses of multiple factors at both global and regional scales. The ability to quantify population distributions with respect to multiple parameters could advance our understanding of complex interactions among the variety of factors that influence human population distribution.

The primary objective of this study is to quantify the relationship between the global-scale spatial distribution of population and some of the geophysical factors that may influence it. Assuming that the spatial distribution of a population is the net result of many different physical, cultural, and socioeconomic factors, we would like to quantify the extent to which some physical environments are more densely populated than others. The presence or absence of patterns in these distributions may indicate the relative importance of physical environmental factors to the large-scale distribution of population. The existence of

such patterns at global, regional, or local scales would have implications for global change scenarios and their potential impact on human populations.

In this study we extend and refine the analysis of Cohen and Small (1998) to consider the spatial distribution of global population with respect to several basic continental physiographic and climatic parameters. The recent availability of global compilations of census and geophysical data allows us to quantify the relationships among these quantities globally at much finer spatial scales than was previously possible. By geographically co-registering these datasets we determine the distribution of population and land area as functions of individual parameters such as proximity to the coast or annual precipitation. We also consider more complex relationships involving multivariate distributions of population and land area to determine what combinations of physical environmental parameters are more densely populated.

## DATA

Spatial distribution of population is provided by the most recent Gridded Population of the World (GPW2) dataset (CIESIN/FPRI/WRI 2000). This dataset represents a significant improvement over the original GPW dataset described by Tobler et al. (1997). Gridded estimates of population count and population density (people/km<sup>2</sup>) are based on a compilation of populations and areas of 127,105 political or administrative units derived from censuses and surveys. (See fig. A). The range of census years used was 1967 to 1998, and all populations were projected to a common base year of 1990 to yield a global population of 5,204,048,442 people. Population counts are assumed to be distributed uniformly within each administrative unit and sampled on a grid of 2.5-arc-minute (2.5') quadrilaterals (Deichmann, Balk, and Yetman 2001). The mass-conserving gridding algorithm is described in more detail by Tobler et al. (1997). These data are available online at [sedac.ciesin.columbia.edu/plue/gpw/index.html](http://sedac.ciesin.columbia.edu/plue/gpw/index.html).

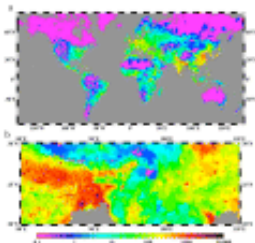


**Fig. A.** Human population distribution at two spatial scales. a, gridded population of the world (GPW2), showing population density on a logarithmic scale. b, regional-scale enlargement of GPW2, showing the variability in the spatial resolution of the administrative units on which the grid is based.

(121 kB)

The spatial resolution of the population dataset is constrained by the size and number of administrative units in the census compilation, which vary among and within countries. More densely populated areas are generally sampled in smaller administrative units (see fig. B). As a result, many more people reside within the smaller administrative units and can therefore be located with greater spatial certainty. The effective spatial resolution of each irregularly shaped unit is proportional to the square root of its area and provides an estimate of the spatial uncertainty in the location of its inhabitants within the unit. The distribution of population as a function of administrative unit size gives an indication of the precision to which the world's human population can be located. The GPW2 dataset allows 50% of the world's population to be located to within 31 km and 90% to within 88 km. This dataset provides adequate spatial detail for a global analysis but would not be appropriate for local analyses at scales below 30 km in many areas. The original GPW dataset

locates 50% to within 63 km and only 14% of the population to within 31 km. The fivefold increase in the number of census estimates results in a significant increase in spatial resolution.

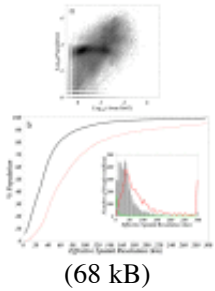


**Fig. B.** Spatial resolution. a, distribution of census data as a function of effective spatial resolution (square root of area in square kilometers) for the 127,105 administrative units in the GPW2 dataset for 1990. Shading indicates exponentially greater numbers of administrative units in darker bins. White strips correspond to unfilled bins resulting from the finite precision of the population and area quantification. b, cumulative spatial resolution of the GPW (lower curve) and GPW2 (upper curve) datasets. The inset histograms show the distribution of population as a function of the effective spatial resolution of the census data used to construct the gridded datasets. Effective spatial resolution indicates the spatial uncertainty in the location of the inhabitants of each administrative unit. The gray histogram shows the distribution for GPW2; the superimposed red curve corresponds to GPW and the superimposed green curve corresponds to units in the U.S.A.

Continental elevations were interpolated from a 5-arc-minute grid derived from global 30-arc-second (30<sup>''</sup>, about 1 km at the equator) gridded elevation estimates provided by the EROS (Earth Resources Observation Systems) Data Center, Sioux Falls, South Dakota. The 30<sup>''</sup> elevation model was derived from Defense Mapping Agency digital terrain elevation data level 1 (3<sup>''</sup>, about 100 m at the equator) gridded topography as well as from data from several other international mapping agencies. The gridded topography covered North and South America, Africa, Europe, Asia, Australia, Oceania, Greenland, and Antarctica. Reduced-resolution representations of the elevation model and links to the contributing datasets are available online at [www.LDEO.columbia.edu/~small/GDEM.html](http://www.LDEO.columbia.edu/~small/GDEM.html).

Coastal proximity was calculated as distance to the nearest coastline at each point for which a population estimate was available. The coastline is based on the Global Self-consistent Hierarchical High Resolution Shoreline (Wessel and Smith 1996) digital coastline file, consisting of 10,390,243 points worldwide. Fluvial proximity was calculated as distance from nearest permanent river as defined by the Digital Chart of the World (DCW 1993). This dataset has limited ability to resolve small tributaries and should not be interpreted as representative of all flowing water sources. Because distances were calculated for a uniform 2.5<sup>l</sup> grid, the cells containing coastline and river points are assigned a proximity of 0 km while proximities of interior grid cells are based on the distance from the centroid of the interior cell to the centroid of the nearest coastal or river cell. This approximation introduces an error of less than one grid cell to the proximity estimates. We accept this introduced uncertainty because the emphasis of this study is on global distributions and because the spatial uncertainties in the population distributions are significantly larger.

Climatic parameters were derived from global climatologies compiled by New, Hulme, and Jones (1999, 2000). Gridded monthly averages of 12,092 temperature and 19,295 precipitation stations compiled over the years 1961 to 1990 were used to calculate annual average and annual range (maximum minus minimum) for each 0.5° grid cell provided by New et al. The annual averages and ranges discriminate the primary climatic divisions observed at global scales. These climatic data do not resolve distinct microclimates that may exist at scales finer than 0.5° (about 55 km at the equator). Other important climatic variables (e.g., wind, frost days, cloud cover, potential evapotranspiration) are not resolved by these data.

We co-registered the demographic and geophysical data by calculating the bilinear interpolant of the

geophysical values surrounding the center of each 2.5' quadrangle for which a population estimate was available. For the elevation data, we averaged the 25 30" elevation estimates corresponding to the area of each 2.5' population estimate. We also estimated population density for each quadrangle. We did not account for differences in the fractional land area of quadrangles on coastlines; in these areas, population densities are minimum estimates. Therefore we could be underestimating coastal population densities.

## SPATIAL LOCALIZATION OF POPULATION

The gridded estimates of population density reveal several contiguous regions with higher population density and larger regions with much lower population densities. The wide range of population densities makes it difficult to appreciate the extent to which a population is localized or dispersed. Small, densely populated areas (cities) can contain many more people than the larger surrounding areas that are more apparent in spatial representations of population distribution. The range of population densities in this dataset spans more than six orders of magnitude, and therefore we display population density on a logarithmic scale to show the range more effectively.

To show the geographic distribution of population over the available land area, we plot a Lorenz curve for the spatial distribution of population in the GPW2 dataset ([fig. 1](#)). This curve will be referred to here as a spatial localization function (SLF) to distinguish it from Lorenz curves describing population distribution with respect to nonspatial parameters. The curvature of the function indicates the degree of spatial localization. A linear localization function depicts a uniform distribution over all available area. A delta function (spike) depicts the concentration of the entire population in the smallest possible land area.

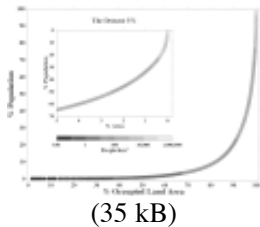


**Fig. 1.** Spatial Lorenz curve for the global human population in 1990, showing the cumulative fraction of the population as a function of the cumulative fraction of enumerated land area (excluding Antarctica and some boreal areas) when units are ordered by increasing population density. The inset shows the most densely populated 5% of land areas with axes inverted. Half the world's population occupies less than 3% of the currently enumerated land area at densities greater than 500 people/ km<sup>2</sup>.

[Figure 1](#) shows that half of Earth's potentially habitable land area is thinly populated, containing < 2% of the human population at densities of less than 10 people /km<sup>2</sup>, while half of Earth's human population experiences high population densities (> 500 people/km<sup>2</sup>) on less than 3% of the potentially habitable land area. For the purposes of this study, we consider all populated areas included in census enumerations to define the potentially habitable land area. The population densities displayed on the Lorenz curve allow different densities to define the threshold of human habitability. The observation that 50% of the population occupies less than 3% of the land area is consistent with the independent estimate that urban areas account for ~2% of Earth's land area (Small [n.d.](#)) and the estimate that almost half the world's population lives in urban areas (United Nations Population Division [2001](#)).

## COMPARATIVE DISTRIBUTIONS OF LAND AREA AND POPULATION

Characteristics of continental physiography such as elevation relative to sea level, proximity to nearest coastline, and proximity to nearest river presumably influence habitation. Other physical factors, such as

climate or ecological zone, also influence human habitation. These physical quantities have restricted distributions over Earth's available land area. For example, the number of people who can live at a particular elevation or climatic zone is constrained by the amount of land area available at that elevation or climate zone. For this reason, we consider the distribution of both population and land area for the geophysical parameters discussed here. (See [figs. C and D](#)). Combinations of factors may influence the spatial distributions of population and land area. Here we limit ourselves to univariate and bivariate distributions of population and land area, but the approach used in this study can be extended to quantification of complex relationships among combinations of parameters. This type of analysis could also be applied to additional, nongeophysical (e.g., socioeconomic and biogeographic) parameters with known geographic distributions.

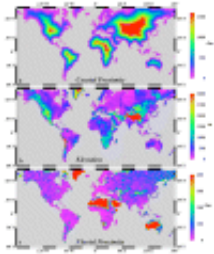


**Fig. C.** Continental physiography as represented by (a) proximity to nearest sea coast, (b) elevation, and (c) proximity to nearest permanent river. Maps are saturated red for values larger than the maximum shown on the scale.

(150 kB)

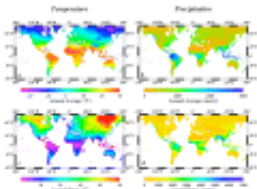


**Fig. D.** Climate as represented by (a) annual average temperature, (b) annual average precipitation rate, (c) annual temperature range, and (d) annual precipitation range. The ranges are differences between the warmest (or wettest) and coldest (or driest) months. Monthly averages are based on the 1961–90 climatology of New, Hulme, and Jones (1999, 2000). Grid resolution is 0.5° in latitude and longitude.

(107 kB)

Some univariate relationships between global population and continental physiography are summarized in [figure 2](#). Population diminishes rapidly with increasing elevation and with increasing distance from coastlines and major rivers. The decrease with increasing distance from rivers would presumably be more pronounced if smaller tributaries were included in the data. The land area distributions show similar patterns, which constrain the land area available for human habitation. Areas and populations outside the range of the plots are incorporated into the extreme bins of the histograms. The ranges were chosen to emphasize the distribution of population. All of the physiographic parameters have ranges extending beyond the population distributions. By contrast, the range of climatic parameters is almost completely spanned by human populations.

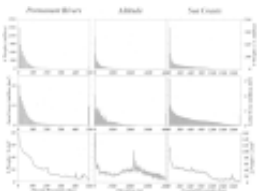


**Fig. 2.** Global distribution of population and land area relative to continental physiographic parameters.

(45 kB)

The proportions of people who live within various distances from a coastline differ slightly according to the GPW2 data from the proportions estimated from the original GPW data. Rounded to the nearest whole

percent, the proportions based on GPW2 for the distances 100, 150, 200, and 400 km (with the proportions based on GPW in parentheses) are 38% (37%), 44% (44%), 50% (49%), and 67% (66%). Given the likely inaccuracies in the data, the differences in the results between the two datasets have little significance.

The visual similarity in the distributions of population and land area conceals the relationship between the population and the parameters. The population distribution can be normalized for the effect of the land area distribution by dividing the number of people at a given elevation (or distance) by the land area at that elevation (or distance) to give the total number of people per square kilometer of land at that elevation (or distance). We refer to this ratio as the integrated population density (IPD) function for that parameter (Cohen and Small 1998). The global IPD for elevation shows pronounced peaks at sea level and at 2,300 m. The densities are comparable ( $> 100$  people/km<sup>2</sup>), but the peak near sea level represents many more people. The peak at 2,300 km is largely a result of the densely populated volcanic highlands of central Mexico.

Univariate relationships between global population, land area, and some climatic parameters (fig. 3) show that population is not as localized with respect to the climatic parameters as it is with respect to the physiographic parameters. The population distribution with respect to temperature shows distinct tropical and temperate peaks, while the distribution with respect to precipitation is unimodal and skewed toward arid climates. Because temperature and precipitation vary appreciably in the course of a year, we consider the temporal variability as the range (maximum minus minimum) of monthly average temperature or precipitation. The direct interdependencies and time-varying component of the climatic parameters require a higher-dimensional analysis to represent the influence of interannual climatic change on population distribution.

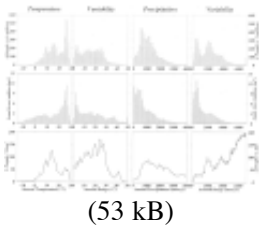
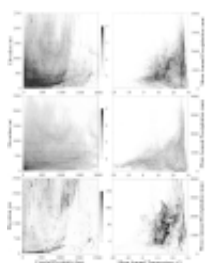


**Fig. 3.** Global distributions of population and land area relative to climatic parameters. The 30-year means of monthly temperature and precipitation estimates are derived from gridded climate data (New, Hulme, and Jones 1999, 2000). In comparison with continental physiographic parameters, population distribution is not strongly localized with respect to any of the climatic parameters. The most prominent features are the low population at average temperatures below 0°C and the pronounced increase in integrated population density (bottom right curve) for annual precipitation ranges greater than 5,000 mm/yr. This peak corresponds to the areas receiving the Asian monsoons.

## POPULATIONS IN MULTIDIMENSIONAL PARAMETER SPACE

Every place on Earth is characterized by some combination of geophysical parameters as well as population density and other nongeophysical parameters. A combination of two or more parameters can be considered a point in a multidimensional parameter space. A single point in parameter space is generally associated with a set of points in geographic space corresponding to all the locations that are characterized by that combination of parameters. Each point in the parameter space is also associated with a distribution of other parameter values that are not included in the dimensions of the parameter space. For example, the places on Earth that are 20 km from a coast and 10 m above sea level and have an annual average temperature of 25°C may receive different amounts of precipitation and have a range of population densities. The univariate distributions are therefore components of multivariate distributions which provide more information. Bivariate distributions for two selected pairs of the physiographic and climatic parameters

discussed above are shown in [figure 4](#).

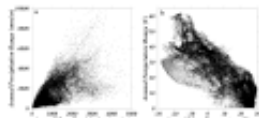


(125 kB)

**Fig. 4.** Global bivariate distributions of population and land area with respect to continental physiography and climate. Left column shows joint distributions of elevation and coastal proximity; right column shows joint distributions of mean annual precipitation and mean annual temperature. First row shows number of people. Second row shows occupied land area. Third row shows integrated population density (people/area). Shading is logarithmic for population and area and linear for integrated density. High integrated population densities are evident at both high and low elevations, but the curvilinear peak at low elevations represents many more people than the more diffuse peaks at high elevations. The elongate peaks in the climatic population distribution correspond to a bimodal distribution of temperate and tropical populations.

Global bivariate distributions of population and land area are quite different for the physiographic and climatic parameters considered here. As with the univariate distributions, the bivariate population distributions are more localized for the physiographic parameters than for the climatic parameters. The bivariate distributions also reveal some patterns not apparent in the univariate distributions. The large number of people at low elevations (< 400 m) is not uniformly distributed with respect to coastal proximity but displays a specific upward-curving trend with distance extending  $\sim 1,000$  km inland. The shape of this curve may result from the topographic gradients of the densely populated river basins worldwide. The many people within < 100 km of coastlines are distributed over a 1,000-m range of elevations. To some extent, this pattern may result from limitations in the resolution of the census data used here. Many areas on the Pacific rim have narrow coastal plains rising rapidly into adjacent mountain ranges within the area of a single census district. The populations of those districts are often localized along the coastal plain rather than uniformly distributed over the full range of elevations. We do not yet know whether this pattern suffices to account for the observed distribution of population over 1,000 m of elevation within < 100 km of coastlines.

The mean values and the ranges of temperature and precipitation are not independent (see [fig. E](#)). In general, the higher the mean annual precipitation, the higher the range of monthly variation in precipitation during a year. By contrast, the higher the annual mean temperature, the lower the range of monthly variation in temperature during a year. Future multivariate analyses of the distribution of population in relation to climatic variables will need to take account of the correlations among these variables.



(59 kB)

**Fig. E.** Ranges and mean values of temperature and precipitation. a, range of mean monthly precipitation (mm/year) as a function of annual average precipitation (mm/year). b, range of mean monthly temperature ( $^{\circ}$ C) as a function of annual average temperature ( $^{\circ}$ C).

## RESULTS AND IMPLICATIONS

The primary conclusion that can be drawn from these simple analyses is that human population is more localized with respect to the physiographic parameters than with respect to the climatic parameters considered here. Even when the distribution of land area is taken into account, there are far more people per available land area within 100 km of coastlines and within 200 m of sea level than farther inland or at higher elevations. In part, this reflects the greater abundance of urban development in coastal zones and along

navigable rivers. Global analysis of stable night light distribution confirms that lighted urban areas occupy a significantly higher fraction of available land area at lower elevations near rivers and sea coasts (Small *n.d.*). Localization along coastlines offers economic and strategic advantages (Smith 1937 [1776], Sachs 1997) as well as proximity to coastal and marine food sources (Walker 1990). Inland localization is consistent with patterns of agricultural development, since the lowest elevations tend to be river valleys and deltas where sediments accumulate to form extensive flat areas of rich soil. This analysis provides quantitative estimates of the distribution of global population relative to coastlines. The resolution of the data is not sufficient to make meaningful statements about the number of people subject to coastal hazard or sea-level rise worldwide (Small et al. 1999), but this analysis does show that some recent estimates are significantly overstated (see Cohen et al. 1998).

While the distributions of population relative to the climatic parameters considered here are not strongly localized at a global scale, the climatic distributions do highlight some interesting patterns. The most prominent climatic localization is the increase in IPD with precipitation variability. As the annual variability in precipitation increases, the land area decreases faster than the number of people. The regions with higher annual variability in precipitation are densely populated areas experiencing the Indian and East Asian monsoons. In comparison with other seasonal precipitation patterns, the monsoons are relatively stable components of the climatic system in the current configuration of continents and oceans. Consistency of precipitation is important for agriculture in areas where irrigation is not feasible. This consistency may facilitate long-term habitation in areas where other factors (such as elevation and drainage) are also conducive to agriculture. In addition to the stability of the monsoons, the densely populated river basins of southern and eastern Asia receive runoff from snowmelt on the Tibetan Plateau. The size and elevation of the plateau guarantee a relatively consistent annual snowpack (and hence runoff) in comparison with smaller, less extensive mountain ranges. Interannual consistency in runoff can offset interannual variability of precipitation in downstream drainage basins, thereby stabilizing the conditions necessary for intensive agriculture. The climatic stability of the monsoons combined with the interannual consistency of runoff may provide a partial explanation for the persistence of large, dense agrarian populations in the Asian river basins (e.g., Huang, He [Yellow], Chang Jiang [Yangtze], Pearl, Song koi [Red], Mekong, Chao Phraya, Ganges-Brahmaputra, Indus).

All of the quantities discussed here are estimates derived from spatial and temporal averages. A more detailed analysis should consider the spatial and temporal scaling of the distributions from which these estimates are derived. Grid resolutions and averaging times are chosen to retain as much information as possible given the resolution of the input data. While these resolutions are appropriate for global and regional analysis, the resolution may be inadequate for more detailed local analyses. Understanding the spatial and temporal scaling properties of these parameters may simplify large, high-dimensional analyses by suggesting optimal measurement scales for some parameters.

A detailed understanding of the relationships between population and environmental parameters such as those shown here requires a more detailed analysis in a high-dimensional parameter space with explicit time dependence. Most global datasets currently available still lack sufficient resolution in either space or time to permit such analysis. Spatiotemporal resolution is a critical consideration for studies of dynamics because



spatial and temporal undersampling of finer-scale variance can corrupt the representation of larger-scale structure.

The methodology described here is not limited to physical parameters. This type of quantitative multidimensional analysis could be extended to various spatially varying cultural and socioeconomic factors that may have equal or greater influence on population distributions and to biogeographic parameters that may be influenced by concentrations of human populations. Other methods of description, modeling, and analysis of these spatial datasets may also prove useful (Bachi 1999, Haining 1990, Longley and Batty 1996).

The results here are an initial step in a larger program of describing and understanding human interactions with Earth's physical, chemical, and biological features. A more detailed comparative analysis of regional distributions could discriminate between the global patterns that are consistently observed at regional and local scales and those that are the product of combinations of disparate regional patterns. One objective is to determine which relationships exhibit spatial and temporal scaling behavior. The next step will be to develop an integrated approach to analyzing joint distributions of all the parameters considered here as well as additional factors such as land-cover class and temporal phase of temperature and precipitation.

It is important to distinguish our efforts to describe the associations between human population density and physical environmental characteristics from the geographical determinism of, for example, Huntington. Our main result—that human population density is, on a global basis, less associated with climatic variables than with elevation and distance from coastlines—argues against the determination of human population density by climatic factors alone. Our aim has been to assess the relative importance and nature of the influences of climatic and physiographic factors rather than to claim that any or all of them are sufficient to account for the global distribution of human population density. The factors we have considered do not include manifestly important social, economic, and historical factors but merely set the stage in which those factors act.

## APPENDIX: MEASUREMENT OF SPATIAL RESOLUTION

One convenient way to measure the spatial resolution of the population assigned to an administrative unit is by the length of the side of a square with the same area as the administrative unit. For a country with  $n$  administrative units, Deichmann, Balk, and Yetman (2001:3) suggest measuring the mean resolution as  $(\text{country area}/n)^{0.5}$ , which is equivalent to  $(\text{sum of unit areas}/n)^{0.5}$ . However, a problem arises because the square root is a nonlinear function. The mean resolution of two (or more) regions or countries is not equal to the mean resolution of the sum of their administrative units. For example, if a country with total area  $C$  consists of two regions with areas  $A$  and  $B$  respectively, where  $C = A + B$ , then in general it is not true that  $(C/2)^{0.5} = (A^{0.5} + B^{0.5})/2$ . We propose a population-weighted measure of spatial resolution that avoids this problem: Mean resolution (km) =  $\frac{\sum_i \text{population in unit } i \times \sqrt{\text{area of unit } i}}{\sum_i \text{population in unit } i}$ . The summations in the numerator and denominator of this formula include all administrative units in the region or country. Moving the square-root function inside the summation guarantees that different combinations of the same administrative units yield the same mean resolution. An area-weighted measure of spatial resolution could be defined similarly by replacing population by area in the sums in both numerator and denominator.

Weighting the resolution measure by population or area accommodates spatial clustering and makes it possible to express spatial uncertainty in terms of the fraction of population or the fraction of area.

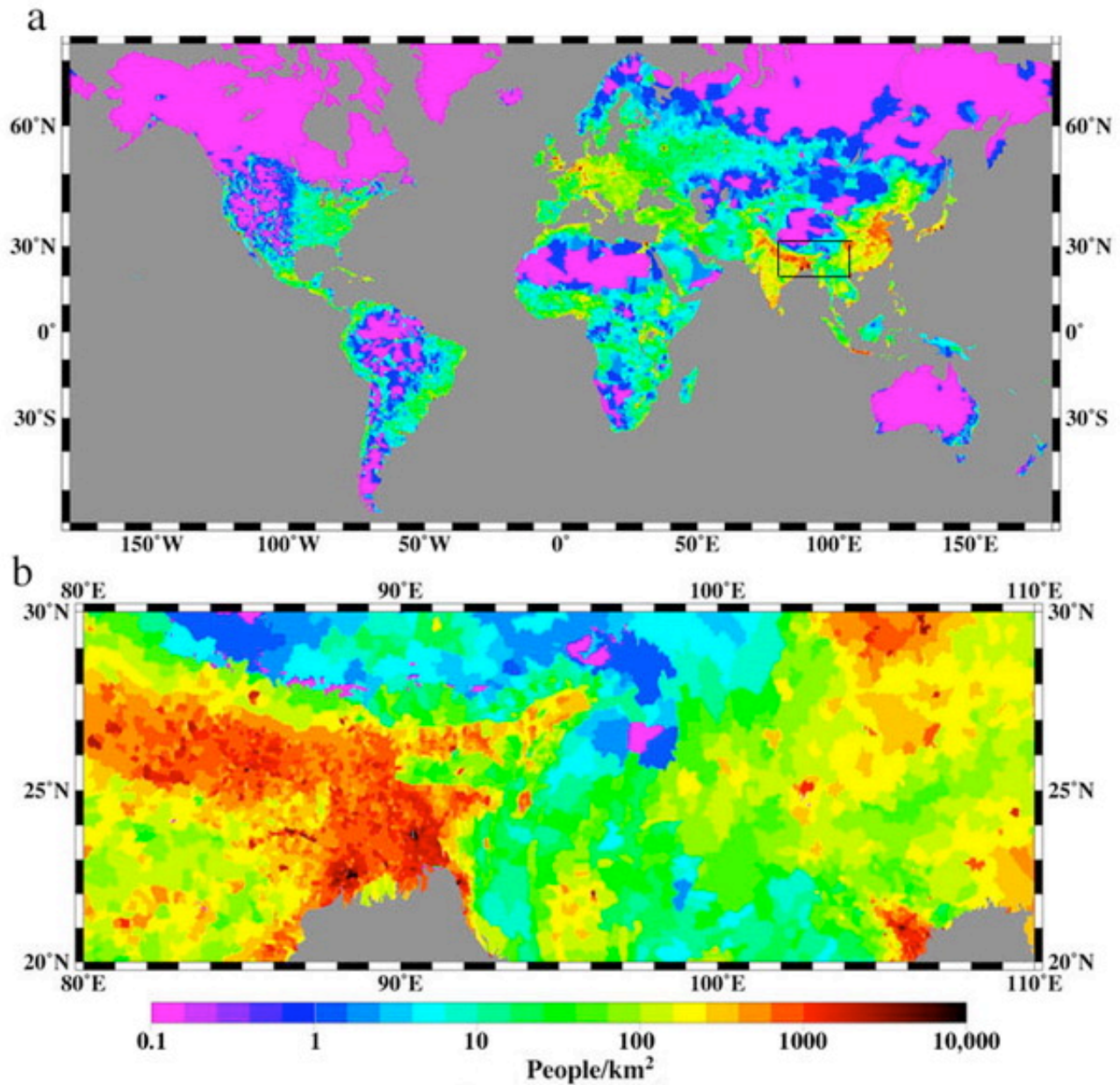
## References Cited

- BACHI, ROBERTO. 1999. *New methods of geostatistical analysis and graphical presentation: Distributions of populations over territories*. New York: Kluwer Academic/Plenum Publishers. [First citation in article](#)
- CIESIN/IFPRI/WRI (CENTER FOR INTERNATIONAL EARTH SCIENCE INFORMATION NETWORK, COLUMBIA UNIVERSITY, INTERNATIONAL FOOD POLICY RESEARCH INSTITUTE, AND WORLD RESOURCES INSTITUTE). 2000. *Gridded population of the world (GPW), Version 2*. Palisades, N.Y. Available at <http://sedac.ciesin.org/plue/gpw/index.html?main.html&2>. [First citation in article](#)
- COHEN, J. E., AND C. SMALL. 1998. Hypsographic demography: The distribution of human population by altitude. *Proceedings of the National Academy of Sciences, U.S.A.* 95(24):14009–4. [First citation in article](#)
- COHEN, J. E., C. SMALL, A. MELLINGER, J. GALLUP, AND J. SACHS. 1998. Estimates of coastal populations. *Science* 278:1211–12. [First citation in article](#)
- DEICHMANN, UWE, D. BALK, AND G. YETMAN. 2001. Transforming population data for interdisciplinary usages: From census to grid. MS, CIESIN. [First citation in article](#)
- DCW (*Digital chart of the world database military specification [mil-d-89009]*). 1993. Philadelphia: Defense Printing Service. Available at <http://www.lib.ncsu.edu/stacks/gis/dcw.html>. [First citation in article](#)
- HAINING, ROBERT P. 1990. *Spatial data analysis in the social and environmental sciences*. Cambridge, U.K., and New York: Cambridge University Press. [First citation in article](#)
- HUNTINGTON, ELLSWORTH. 1915. *Civilization and climate*. New Haven: Yale University Press. [First citation in article](#)
- ———. 1921. *Principles of human geography*. New York: Wiley. [First citation in article](#)
- ———. 1924. 3d edition, revised and rewritten. *Civilization and climate*. New Haven: Yale University Press. [First citation in article](#)
- ———. 1927. *The human habitat*. New York: D. Van Nostrand. [First citation in article](#)
- ———. 1951. 6th edition. *Principles of human geography*. New York: Wiley. [First citation in article](#)
- ———. 1963. *The human habitat*. New York: W. W. Norton. [First citation in article](#)
- KATES, R. W., B. L. TURNER, AND W. C. CLARK. 1990. "The great transformation," in *The earth as transformed by human action: Global and regional changes in the biosphere over the past 300 years*. Edited by B. L. Turner, W. C. Clark, R. W. Kates, J. F. Richards, J. T. Mathews, and W. B. Meyer, pp. 1–17. Cambridge: Cambridge University Press with Clark University. [First citation in article](#)
- KING, G., G. BAILEY, AND D. STURDY. 1994. Active tectonics and human survival strategies. *Journal of Geophysical Research* 99:20063–78. [First citation in article](#) | [CrossRef](#)
- LONGLEY, PAUL, AND MICHAEL BATTY. 1996. *Spatial analysis: Modeling in a GIS environment*. Cambridge, U.K.: GeoInformation International (Pearson Professional). [First citation in article](#)
- NEW, M. G., M. HULME, AND P. D. JONES. 1999. Representing twentieth-century space-time climate variability. Pt. 1. Development of a 1961–1990 mean monthly terrestrial climatology. *Journal of Climate* 12:829–56. [First citation in article](#) | [CrossRef](#)
- ———. 2000. Representing twentieth-century space-time climate variability. Pt. 2. Development of a 1901–1996 monthly terrestrial climate field. *Journal of Climate* 13:2217–38. [First citation in article](#) | [CrossRef](#)
- SACHS, J. 1997. The limits of convergence: Nature, nurture, and growth. *Economist*, June 14, pp. 19–22. [First citation in article](#)
- SEMPLE, E. C. 1911. *Influences of geographic environment*. New York: Henry Holt. [First citation in article](#)
- SMALL, C. n.d. "Physical environment and the spatial distribution of human population," in *The*

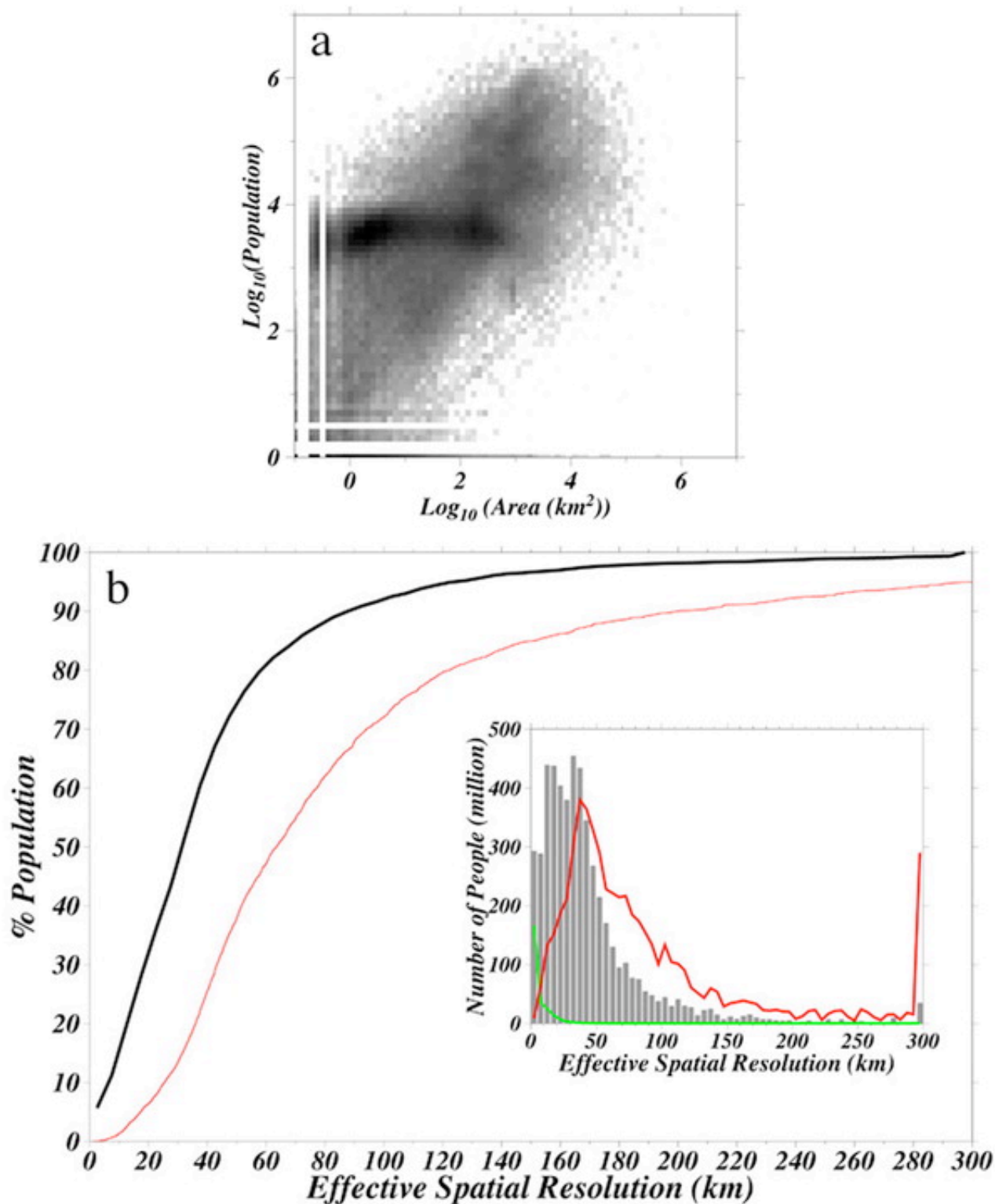
*demography and geography of Homo sapiens and its implications for biological diversity*. Edited by Richard P. Cincotta and Deirdre Mageean. MS. [First citation in article](#)

- SMALL, C., V. GORNITZ, AND J. E. COHEN. 1999. Coastal hazards and the global distribution of human population. *Environmental Geosciences* 7(1):3–12. [First citation in article](#) | [CrossRef](#)
  - SMITH, ADAM. 1937 (1776). *An inquiry into the nature and causes of the wealth of nations*. Edited by Edwin Cannan. New York: Modern Library. [First citation in article](#)
  - TOBLER, W., U. DEICHMANN, J. GOTTSEGEN, AND K. MALOY. 1997. World population in a grid of spherical quadrilaterals. *International Journal of Population Geography* 3:203–25. [First citation in article](#) | [CrossRef](#)
  - UNITED NATIONS POPULATION DIVISION. 2001. *World urbanization projects: The 1999 revision*. ST/ESA/SER.A/194. New York. [First citation in article](#)
  - VERNADSKY, W. I. 1929. *La biosphere*. Paris: Felix Alcan. [First citation in article](#)
  - VITOUSEK, P., H. A. MOONEY, J. LUBCHENCO, AND J. M. MELILLO. 1997. Human domination of Earth's ecosystems. *Science* 277:494–99. [First citation in article](#) | [CrossRef](#)
  - WALKER, H. J. 1990. "The coastal zone," in *The earth as transformed by human action: Global and regional changes in the biosphere over the past 300 years*. Edited by B. L. Turner, W. C. Clark, R. W. Kates, J. F. Richards, J. T. Mathews, and W. B. Meyer, pp. 271–94. Cambridge: Cambridge University Press with Clark University. [First citation in article](#)
  - WESSEL, P., AND W. H. F. SMITH. 1996. A global self-consistent, hierarchical, high-resolution shoreline database. *Journal of Geophysical Research* 101 (B4):8741–43. [First citation in article](#)
-

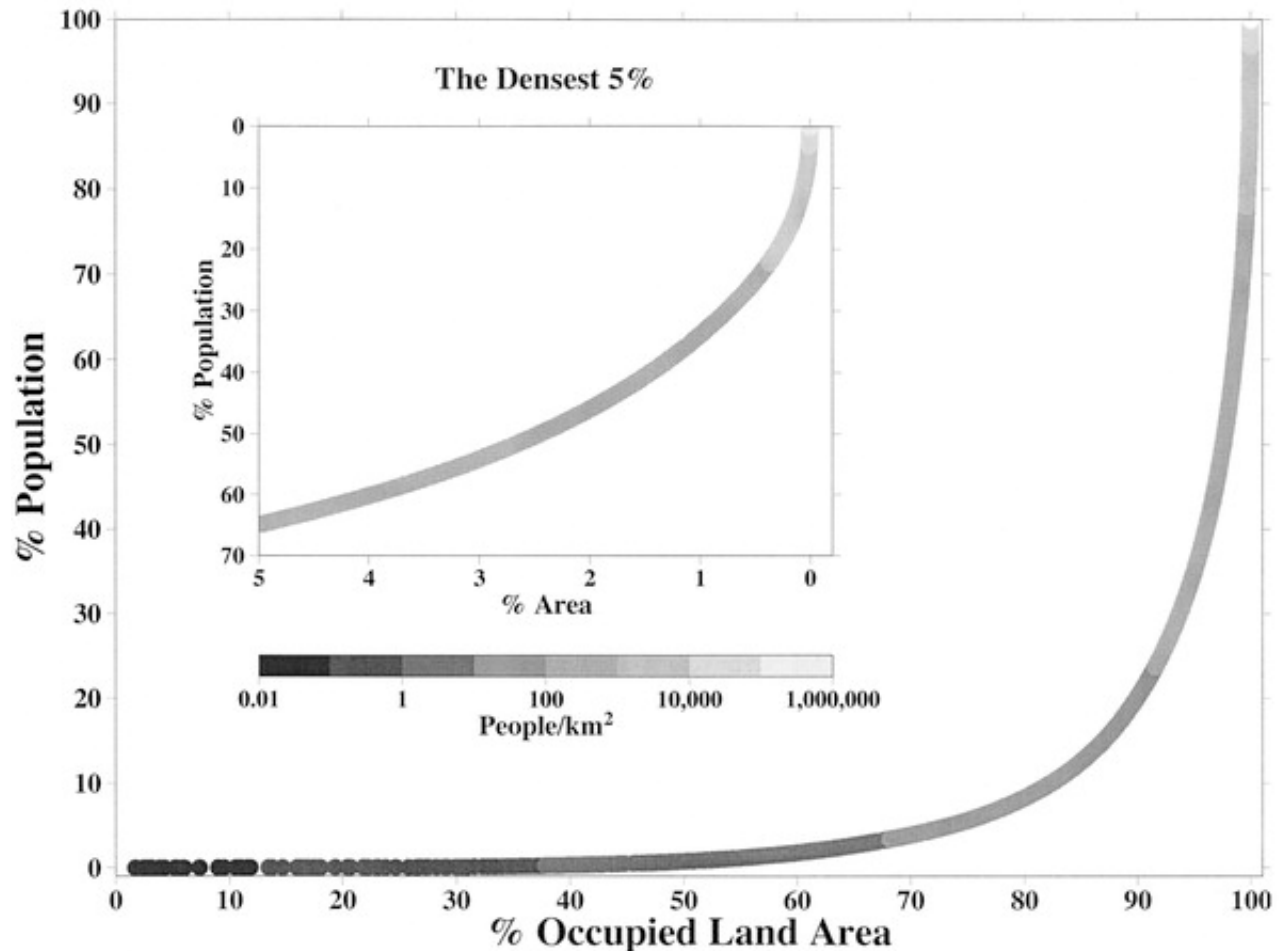
Human population distribution at two spatial scales. a, gridded population of the world (GPW2), showing population density on a logarithmic scale. b, regional-scale enlargement of GPW2, showing the variability in the spatial resolution of the administrative units on which the grid is based.



Spatial resolution. a, distribution of census data as a function of effective spatial resolution (square root of area in square kilometers) for the 127,105 administrative units in the GPW2 dataset for 1990. Shading indicates exponentially greater numbers of administrative units in darker bins. White strips correspond to unfilled bins resulting from the finite precision of the population and area quantification. b, cumulative spatial resolution of the GPW (lower curve) and GPW2 (upper curve) datasets. The inset histograms show the distribution of population as a function of the effective spatial resolution of the census data used to construct the gridded datasets. Effective spatial resolution indicates the spatial uncertainty in the location of the inhabitants of each administrative unit. The gray histogram shows the distribution for GPW2; the superimposed red curve corresponds to GPW and the superimposed green curve corresponds to units in the U.S.A.

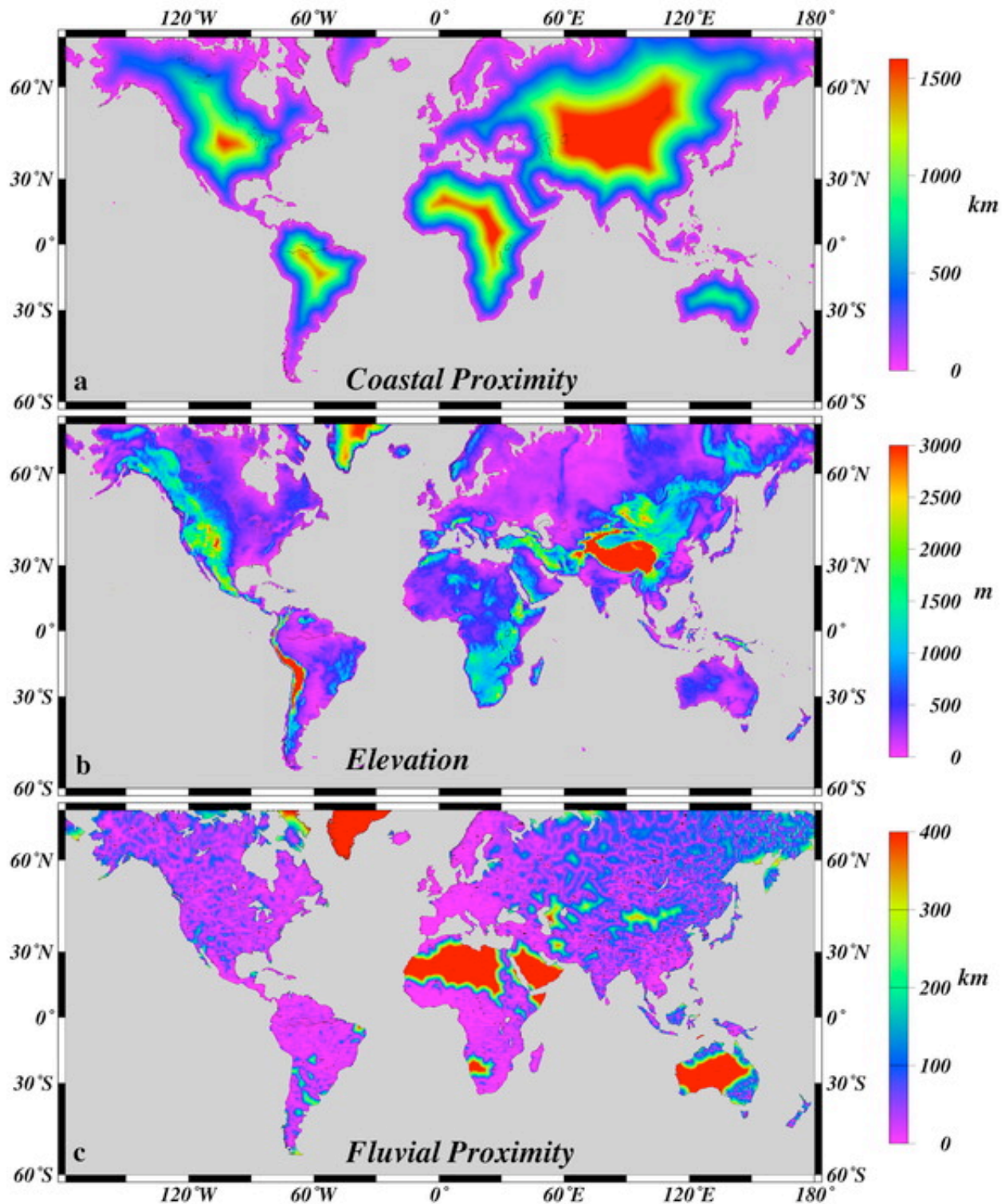


Spatial Lorenz curve for the global human population in 1990, showing the cumulative fraction of the population as a function of the cumulative fraction of enumerated land area (excluding Antarctica and some boreal areas) when units are ordered by increasing population density. The inset shows the most densely populated 5% of land areas with axes inverted. Half the world's population occupies less than 3% of the currently enumerated land area at densities greater than 500 people/ km<sup>2</sup>.



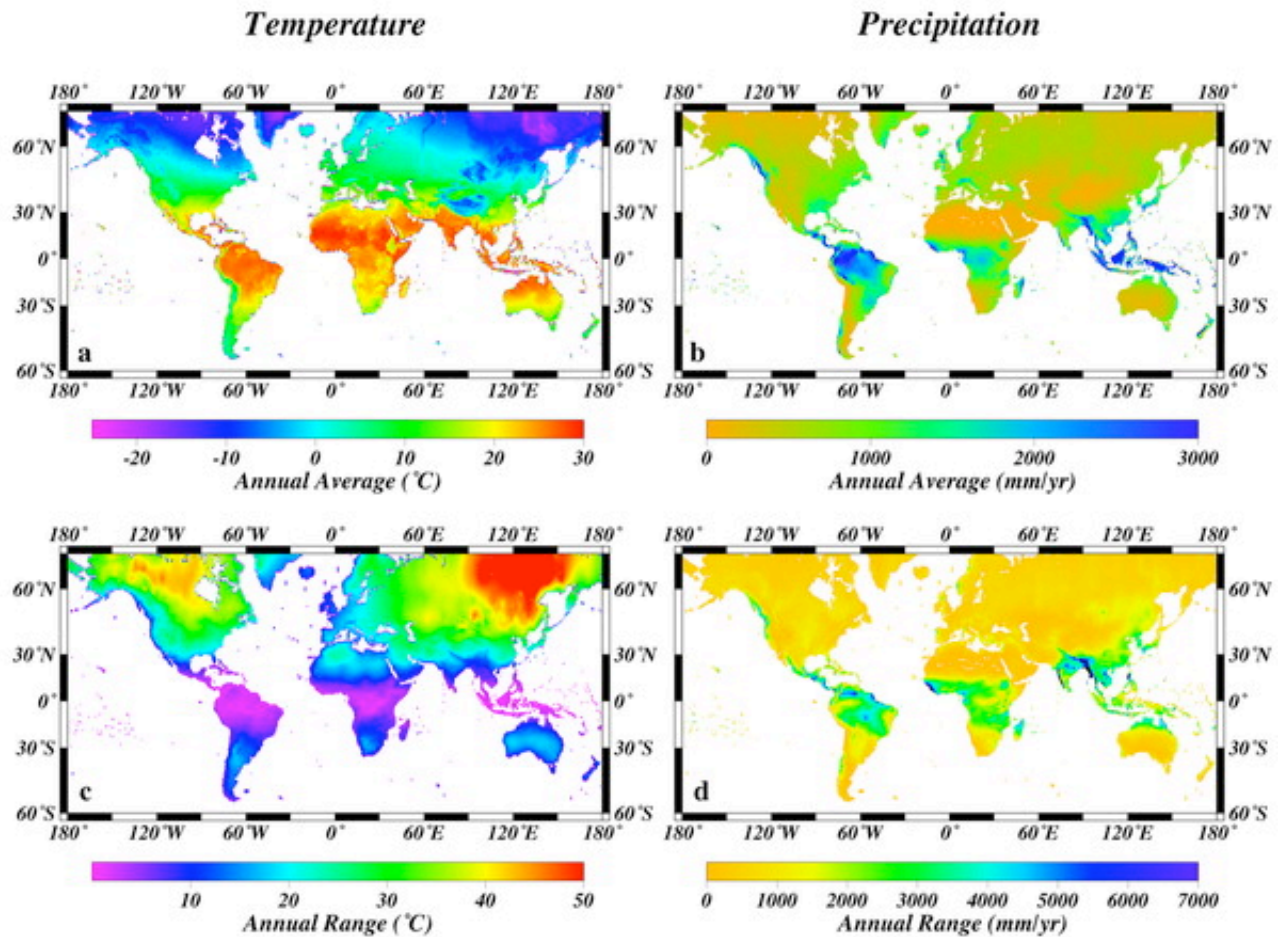


Continental physiography as represented by (a) proximity to nearest sea coast, (b) elevation, and (c) proximity to nearest permanent river. Maps are saturated red for values larger than the maximum shown on the scale.





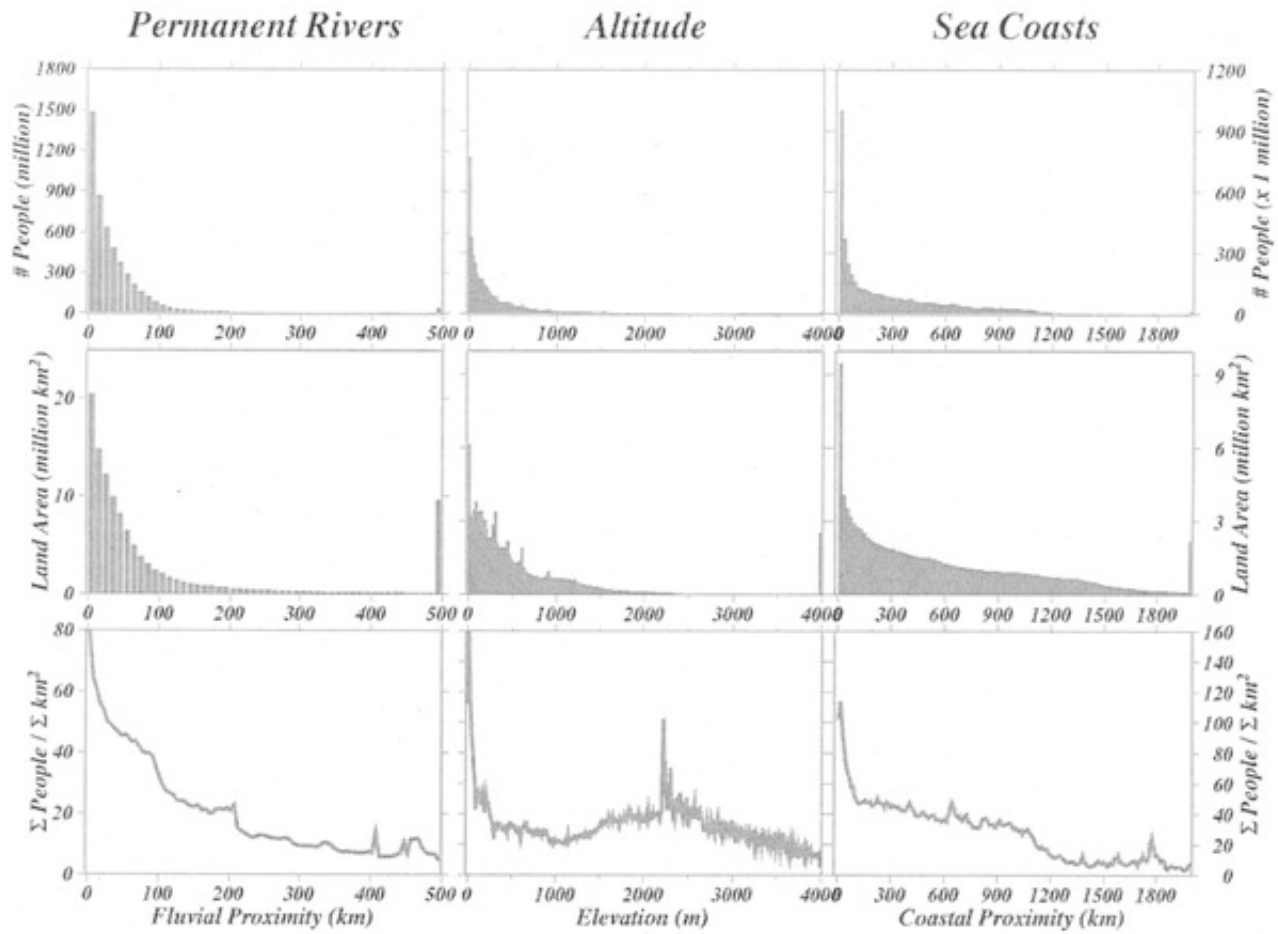
Climate as represented by (a) annual average temperature, (b) annual average precipitation rate, (c) annual temperature range, and (d) annual precipitation range. The ranges are differences between the warmest (or wettest) and coldest (or driest) months. Monthly averages are based on the 1961–90 climatology of New, Hulme, and Jones (1999, 2000). Grid resolution is  $0.5^\circ$  in latitude and longitude.



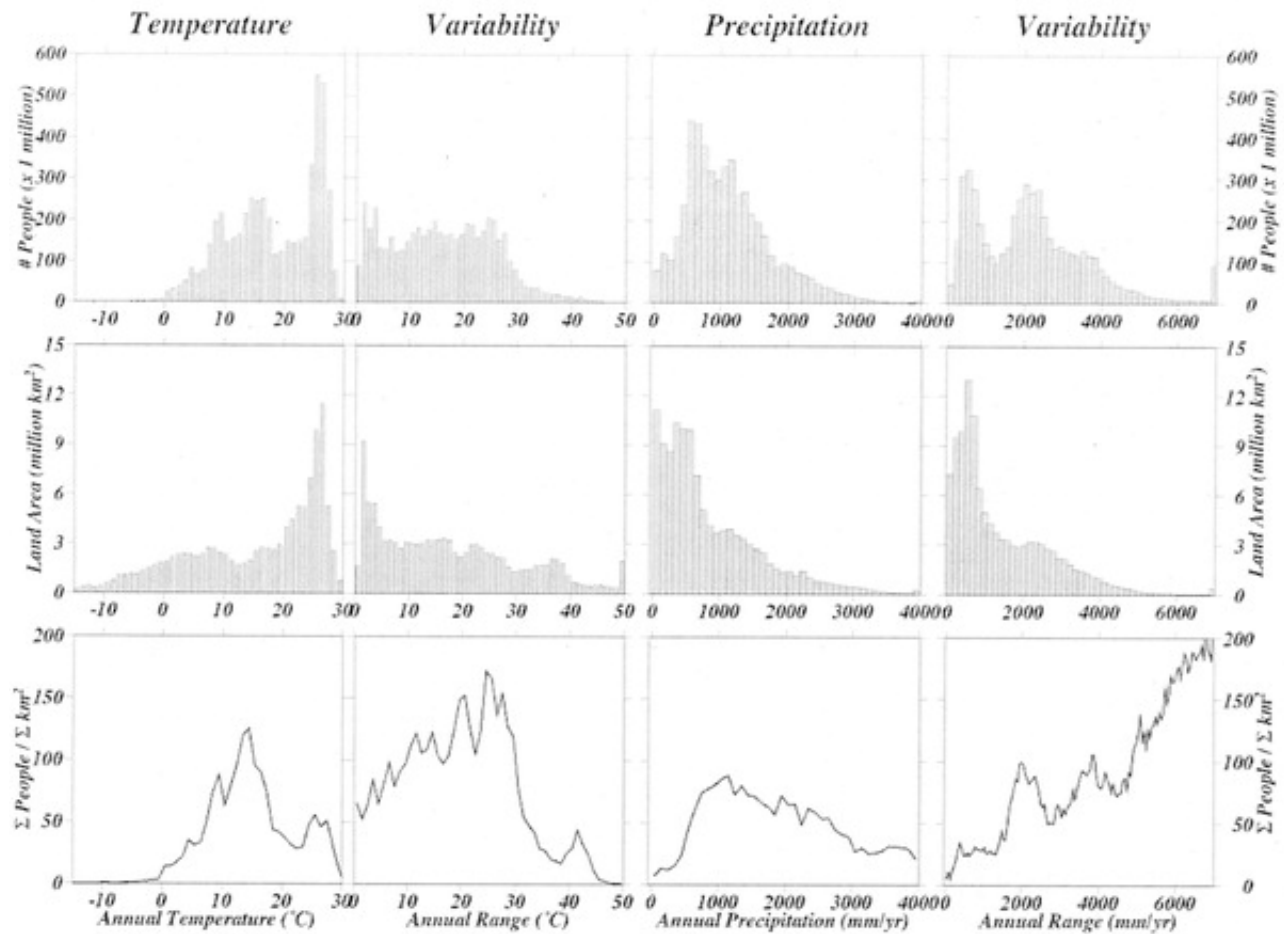




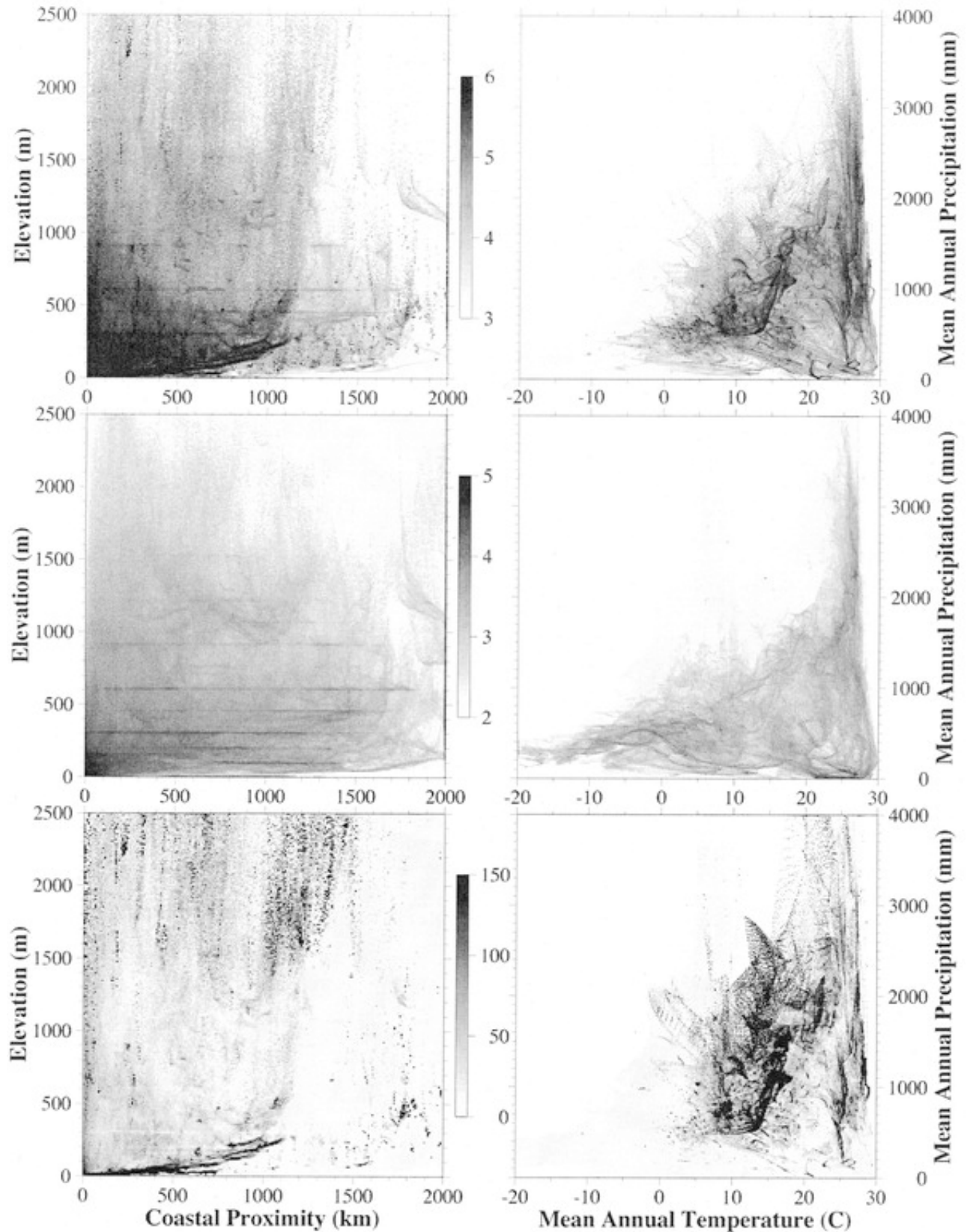
Global distribution of population and land area relative to continental physiographic parameters.



Global distributions of population and land area relative to climatic parameters. The 30-year means of monthly temperature and precipitation estimates are derived from gridded climate data (New, Hulme, and Jones 1999, 2000). In comparison with continental physiographic parameters, population distribution is not strongly localized with respect to any of the climatic parameters. The most prominent features are the low population at average temperatures below 0°C and the pronounced increase in integrated population density (bottom right curve) for annual precipitation ranges greater than 5,000 mm/yr. This peak corresponds to the areas receiving the Asian monsoons.



Global bivariate distributions of population and land area with respect to continental physiography and climate. Left column shows joint distributions of elevation and coastal proximity; right column shows joint distributions of mean annual precipitation and mean annual temperature. First row shows number of people. Second row shows occupied land area. Third row shows integrated population density (people/area). Shading is logarithmic for population and area and linear for integrated density. High integrated population densities are evident at both high and low elevations, but the curvilinear peak at low elevations represents many more people than the more diffuse peaks at high elevations. The elongate peaks in the climatic population distribution correspond to a bimodal distribution of temperate and tropical populations.





Ranges and mean values of temperature and precipitation. a, range of mean monthly precipitation (mm/year) as a function of annual average precipitation (mm/year). b, range of mean monthly temperature ( $^{\circ}\text{C}$ ) as a function of annual average temperature ( $^{\circ}\text{C}$ ).

